


RESEARCH ARTICLE

Self-regulation of ventromedial prefrontal cortex activation using real-time fMRI neurofeedback—Influence of default mode network

Ahmad Mayeli^{1,2} | Masaya Misaki¹ | Vadim Zotev¹ | Aki Tsuchiyagaito^{1,3,4} |
 Obada Al Zoubi^{1,2} | Raquel Phillips¹ | Jared Smith¹ | Jennifer L. Stewart¹ |
 Hazem Refai² | Martin P. Paulus¹ | Jerzy Bodurka^{1,5} 

¹Laureate Institute for Brain Research, Tulsa, Oklahoma

²Electrical and Computer Engineering Department, University of Oklahoma, Tulsa, Oklahoma

³Japan Society for the Promotion Science, Tokyo, Japan

⁴Research Center for Child Development, Chiba University, Chiba, Japan

⁵Stephenson School of Biomedical Engineering, University of Oklahoma, Tulsa, Oklahoma

Correspondence

Jerzy Bodurka, Laureate Institute for Brain Research, Tulsa, OK.

Email: jbodurka@laureateinstitute.org

Funding information

National Institutes of Health; National Institute of General Medical Sciences; William K. Warren Foundation

Abstract

The ventromedial prefrontal cortex (vmPFC) is involved in regulation of negative emotion and decision-making, emotional and behavioral control, and active resilient coping. This pilot study examined the feasibility of training healthy subjects ($n = 27$) to self-regulate the vmPFC activity using a real-time functional magnetic resonance imaging neurofeedback (rtfMRI-nf). Participants in the experimental group (EG, $n = 18$) were provided with an ongoing vmPFC hemodynamic activity (rtfMRI-nf signal represented as variable-height bar). Individuals were instructed to raise the bar by self-relevant value-based thinking. Participants in the control group (CG, $n = 9$) performed the same task; however, they were provided with computer-generated sham neurofeedback signal. Results demonstrate that (a) both the CG and the EG show a higher vmPFC fMRI signal at the baseline than during neurofeedback training; (b) no significant positive training effect was seen in the vmPFC across neurofeedback runs; however, the medial prefrontal cortex, middle temporal gyri, inferior frontal gyri, and precuneus showed significant decreasing trends across the training runs only for the EG; (c) the vmPFC rtfMRI-nf signal associated with the fMRI signal across the default mode network (DMN). These findings suggest that it may be difficult to modulate a single DMN region without affecting other DMN regions. Observed decreased vmPFC activity during the neurofeedback task could be due to interference from the fMRI signal within other DMN network regions, as well as interaction with task-positive networks. Even though participants in the EG did not show significant positive increase in the vmPFC activity among neurofeedback runs, they were able to learn to accommodate the demand of self-regulation task to maintain the vmPFC activity with the help of a neurofeedback signal.

KEYWORDS

brain, default mode network, emotion, fMRI Neurofeedback, functional connectivity, self-regulation, vmPFC

This is an open access article under the terms of the Creative Commons Attribution-NonCommercial License, which permits use, distribution and reproduction in any medium, provided the original work is properly cited and is not used for commercial purposes.

© 2019 The Authors. *Human Brain Mapping* published by Wiley Periodicals, Inc.

1 | INTRODUCTION

Real-time fMRI neurofeedback (rtfMRI-nf) experiments are employed to help individuals learn how to upregulate or downregulate hemodynamic activity of a target brain region in real time. In such experiments, a visual representation of measured blood oxygenation level-dependent (BOLD) signal from the target brain region is used as the reward or reinforcement, such as with a bar notifying an individual of successful regulation (Christopher deCharms, 2008; Christopher deCharms et al., 2005). Beyond defining targets for noninvasive modulation and showing target engagement, rtfMRI-nf has the potential to help subjects train their ability to cope with stress, depression, or anxiety states and may render these individuals more capable of managing stressful situations in the future. Thus, a subset of neurofeedback-fMRI studies have focused on modulating brain areas that are important for processing emotions. A growing literature demonstrates that individuals can successfully regulate BOLD signal within: (a) deep brain structures such as the amygdala (Johnston et al., 2010; Posse et al., 2003; Young et al., 2017; Zotev et al., 2011; Zotev et al., 2018b; Zotev et al., 2014), insula (Berman et al., 2013; Caria et al., 2007; Caria et al., 2010; Rance et al., 2014), thalamus (Zotev et al., 2018b), and anterior cingulate cortex (Weiskopf et al., 2003); (b) primary motor/somatosensory, auditory, and visual cortices for recovery and rehabilitation from neurological disorders (Berman et al., 2012; Haller et al., 2013; Shibata et al., 2011; Yoo & Jolesz, 2002); and (c) regions of the frontal lobe including dorsolateral prefrontal cortex (DLPFC) and orbitofrontal cortex (OFC) (Scheinost et al., 2013; Sherwood et al., 2016). These and other studies indicate that individuals are able to successfully regulate their BOLD signal within these regions and that this regulation is associated with changes in subjective states such as reductions in depression or anxiety symptoms (Young et al., 2017; Zotev et al., 2018b).

The ventromedial prefrontal cortex (vmPFC) has been investigated extensively using neuroimaging and lesion-based approaches and is profoundly important for a number of psychiatric conditions. Specifically, vmPFC is associated with three domains of functions, including (a) the representation of reward (Bartra et al., 2013), subjective value (Brosch & Sander, 2013; Clithero & Rangel, 2013), and value-based decision-making (Bechara et al., 1997; Bechara et al., 2000; Bechara et al., 1996; Damasio, 1996); (b) the generation and regulation of emotion (Hare et al., 2009; Yu et al., 2017), including effective foresight based on previous experience (Benoit et al., 2014); and (c) various aspects of social cognition (Hiser & Koenigs, 2018) including empathy (Janowski et al., 2012). Taken together, these and other studies (e.g., Sinha et al., 2016) highlight the importance of the modulatory role of this brain area for regulating coping with aversive conditions as well as integrating valence-based information to aid goal-directed activity. Besides the association of the vmPFC with emotion control, the vmPFC is part of the default mode network (DMN), an interconnected set of brain areas coactivated at brain wakeful rest and involved with internal reflection and self-awareness, thereby distinguishing vmPFC functionality from that of other frontal brain regions involved more in external executive control (e.g., DLPFC and

OFC). The feasibility of modulating the entire DMN (including vmPFC) activity was investigated in a recent neurofeedback study (McDonald et al., 2017).

Because of the vmPFC involvement in multiple cognitive functions and emotions processing, not surprisingly, this region is also implicated in the pathophysiology of a number of psychiatric disorders. For example, inadequate vmPFC modulation during various task-based and resting-state fMRI recordings is evident in individuals with major depressive disorder (MDD) (Johnstone et al., 2007), posttraumatic stress disorder (PTSD) (Milad et al., 2009), and other anxiety disorders (Burghy et al., 2012). As for the relationship between activity of the vmPFC and subjective state, healthy individuals show attenuated vmPFC BOLD signal during anticipatory anxiety (Simpson et al., 2001), whereas vmPFC also appears to be involved in heightened reappraisal of negative emotion (Bhanji & Delgado, 2014). Taken together, successful vmPFC modulation could help to strengthen a healthy individual's ability to better cope with stressful events, and it may also have important applications for individuals with mood and anxiety disorders.

Due to the crucial role of vmPFC in emotional processing and internal reflection, the present pilot study examined the feasibility of training healthy human subjects to self-regulate vmPFC BOLD signal using active versus sham rtfMRI-nf. We divided the subjects into two groups: (a) the experimental group (EG) received moment-to-moment feedback regarding their current vmPFC BOLD signal; and (b) the control group (CG) received random (sham) computer-based feedback unrelated to their actual vmPFC BOLD signal.

2 | METHODS

2.1 | Human subjects

This study was conducted at the Laureate Institute for Brain Research with the research protocol (IRB# 20111188) approved by the Western Institutional Review Board. All participants were recruited from the community using general advertisements for participating in studies at the Laureate Institute for Brain Research and underwent screening evaluations. All volunteers provided written informed consent and received financial compensation for participation in the study.

The study included 27 medically and psychiatrically healthy volunteers (mean age 29 years, 14 female), after excluding six subjects with excessive motion, falling asleep during scanning, or not complying with instruction. All participants were naive to rtfMRI-nf and were assigned to either EG ($n = 18$) or CG ($n = 9$). Participants in EG were provided with ongoing information about vmPFC BOLD activity and were instructed to raise the BOLD signal by thinking about things that are important to them. We adopted this mental strategy because vmPFC is related to subjective value (Brosch & Sander, 2013; Clithero & Rangel, 2013) and value-based decision-making (Bechara et al., 1996; Bechara et al., 1997; Bechara et al., 2000; Damasio, 1996), and this strategy was estimated to enhance vmPFC BOLD signal. We assigned the same task to CG participants; however, they received computer-generated sham feedback, calculated using a linear combination of seven Legendre polynomials with randomly selected

coefficients (Zotev et al., 2018a). We employed this strategy for the sham signal because the vmPFC is part of the DMN and has extensive anatomical and functional connections with subcortical and cortical brain regions, which makes providing sham feedback from another brain region problematic. The computer-generated sham feedback has been previously successfully deployed (Zotev et al., 2018a) and helps avoid interpretation ambiguities related to vmPFC functional connections between additional brain regions.

2.2 | Data acquisition

Experiments were performed using GE MR750 3T MRI scanner with the 32-channel receive-only head coil. For the whole-brain fMRI recording, a single-shot gradient echo planar image (EPI) with sensitivity encoding (SENSE) (Pruessmann et al., 1999) with FOV/slice = 240/2.9 mm, TR/TE = 2000/30 ms, SENSE acceleration $R = 2$, 96×96 , flip = 90° , 34 axial slices was employed. To allow the fMRI signal to reach a steady state, three EPI volumes (6 s) were added at the beginning of the run and were excluded from data analysis. The fMRI voxel size was $1.875 \times 1.875 \times$

2.9 mm^3 . Eight fMRI runs lasted for 6 min 40 s were collected. In order to acquire an anatomical image, we used a T1-weighted magnetization-prepared rapid gradient echo (MPRAGE) pulse sequence accelerated with SENSE. The parameters for MPRAGE sequence are as follows: FOV = 240 mm, axial slices per slab = 128, slice thickness = 1.2 mm, image matrix size = 256×256 , TR/TE = 5.0/1.9 ms, SENSE acceleration factor $R = 2$, flip angle = 10° , delay time TD = 1,400 ms, inversion time TI = 725 ms, sampling bandwidth = 31.2 kHz, scan time = 4 min 58 s. Physiological pulse oximetry and respiration waveforms were recorded simultaneously with fMRI (with 25 ms sampling interval) using a photoplethysmograph placed on the subject's finger and a pneumatic respiration belt, respectively.

2.3 | Experimental paradigm and protocol

The vmPFC region-of-interest (ROI) target location (spherical ROI, 7 mm radius) shown in Figure 1a was selected based on a meta-analysis results (Clithero & Rangel, 2013) and was centered at the vmPFC ($-2, 35, \text{ and } -3$; Talairach coordinates) (Talairach & Tournoux,

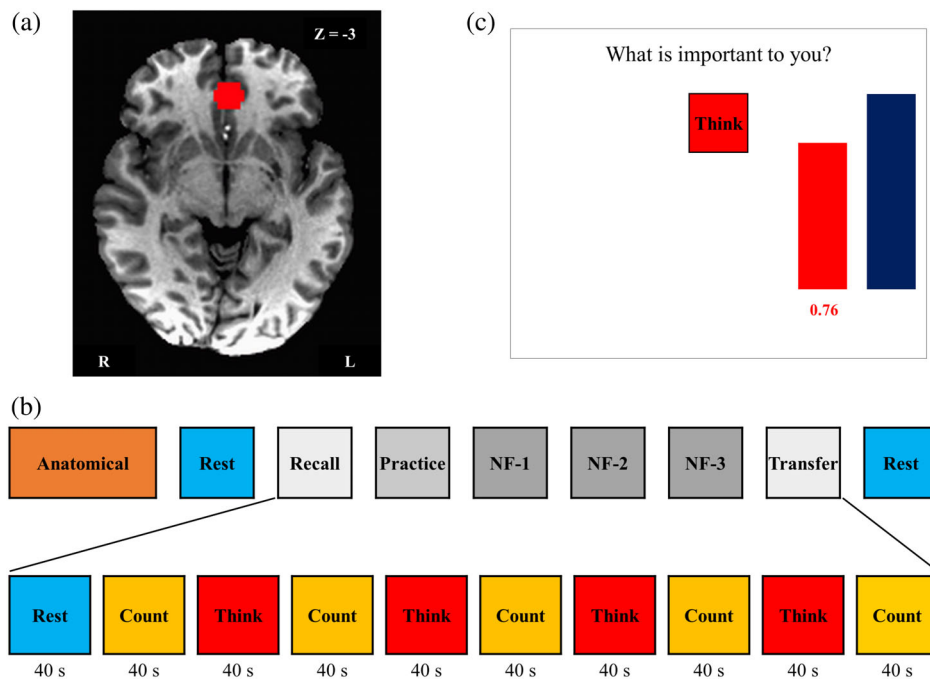


FIGURE 1 Real-time fMRI neurofeedback experiment summary. (a) Region of interest (ROI, spheres of 7 mm radius) for the rtfMRI neurofeedback (rtfMRI-nf) training. Ventromedial prefrontal cortex (vmPFC, Talairach coordinate: $-2, 35, \text{ and } -3$) was selected as the targeted ROI for experimental group. (b) The experimental protocol for neurofeedback training. The experiment consisted of eight fMRI runs each lasting 6 min 40 s. During Rest runs, the participants were instructed to clear their minds and not to think about anything in particular while fixating at the display screen. During Recall (RE) and Transfer (TR) runs, the participants tried to think about the things that are important for them without any feedback. The Practice (PR) run provided the subjects an opportunity to become comfortable with the rtfMRI-nf procedure. During neurofeedback (NF) runs 1–3, the participant underwent rtfMRI-nf training. Each run (except for Rest runs) started with a 40 s rest block, proceeding with a 40 s long block with the Think and Count conditions. The target level (blue bar) was raised from run to run. No neurofeedback was provided (no bars displayed) during the Rest and Count conditions or during the entire RE and TR runs. (c) Graphical user interface (GUI) screen with neurofeedback bars (red) and target bars (blue) during the Think condition. For the Think condition, the subjects were asked to, first, think about thoughts that are important for them that were specific, vivid, and highly arousing in order to activate vmPFC, and then try to increase the level of the red bar to a given blue target level (not necessarily exceeding that target level)

1988). For each subject, this ROI was transformed to the EPI image space using subject's high-resolution MPRAGE T1-weighted structural data.

The study experiment design is shown in Figure 1b. Before scanning, detailed instructions and the experimental paradigm design were presented to participants. Figure 1b shows the order of MRI runs 1–9 consisted of: Anatomical scan; Rest-1; Recall (RE); Practice (PR); three Neurofeedback trainings (NF-1, NF-2, and NF-3); Transfer (TR); and Rest-2. During Rest-1 and Rest-2, a resting-state paradigm was employed, and participants were instructed to clear their minds and not think about anything in particular while fixating upon the display screen. Figure 1b also shows that the six runs (RE, Practice, NF-1, NF-2, NF-3, and TR) started with a 40 s rest block, followed by alternating Count and Think blocks (40 s each; five Count and four Think blocks). During the Count condition, participants were asked to count backward in their mind by subtracting the number shown on the screen. The Count condition (i.e., the control condition) was included to distract participants' attention from contemplating important thought and to dampen the activation of vmPFC. Furthermore, the percent BOLD signal change used in analysis was based on the signal change during the Think condition versus the Count condition. During the Think condition, participants were instructed to think about things that are important to them that were specific, vivid, and highly arousing in order to activate the vmPFC (Clithero & Rangel, 2013) and potentially help them learn to control the level of activity in the target brain region (shown as height of the red bar, Figure 1c). Prior to scanner entry, they were asked to write down five things that matched all—or at least many—of the following features: (a) What they like; (b) What they are good at; (c) What gets them excited; (d) What impresses other people; and (e) What makes them appreciate others. Participants kept answers to these five queries to themselves, but were asked to choose three out of five thoughts to employ starting at the PR run.

During RE and TR runs, the participants were instructed to think about things important for them without any feedback while they saw red box telling them “Think” (Figure 1c). The PR run provided subjects with an opportunity to become familiar with the rtfMRI-nf procedure, helping participants: (a) feel comfortable with the neurofeedback condition inside the scanner; (b) evaluate the emotional impact of the three prepared thoughts that are important for them within the experimental setting; and (c) practice switching from one thought to another during neurofeedback training. During PR, NF-1, NF-2, and NF-3, the participant underwent rtfMRI-nf training so as to raise the level of the red bar displayed on the screen and match to the level of the blue bar during Think condition. Based on our preliminary experiments before starting this study, some participants could increase vmPFC BOLD signal as high as 2% from baseline. Therefore, the target level (i.e., blue bar height) was set as follows: 0.5%, 1.0%, 1.5%, and 2.0% for PR, NF-1, NF-2, and NF-3, respectively. No neurofeedback was provided (no bars displayed) during the Rest and Count conditions or during the entire RE and TR runs. For PR, unlike NF-1, NF-2, and NF-3, the participants were asked to recall the first thought that they wrote down before the experiment for the first

Think block, the second thought for the second Think block, and third thought for the third Think block. For the last Think block, they were instructed to practice one of those three that worked best for them one more time. During Think blocks for Runs 1–3, participants were free to choose any thought that they considered working well for them based on their experiences in PR.

The neurofeedback stimulus was delivered via our custom rtfMRI system (Bodurka & Bandettini, 2008) utilizing the real-time features of Analysis of Functional NeuroImages (AFNI) (Cox & Jesmanowicz, 1999) and custom-developed graphical user interface software. AFNI real-time plug-ins were used to perform volume registration of EPI images in our neurofeedback implementation and to export mean values of fMRI BOLD signals for the vmPFC ROI in real time. The subjects in EG received feedback from the percent signal BOLD change during each Think condition, relative to the baseline obtained by averaging the fMRI signal for the preceding 40 s long Count condition. This neurofeedback bar (percent signal change) was updated every 2 s and displayed on the screen as the red bar (Figure 1c). A moving average of the current and two preceding fMRI percent signal change values was used to reduce the bar fluctuation as explained in (Zotev et al., 2011). As aforementioned, participants in CG received computer-based random feedback. The sham feedback signal, for each condition block, was generated using a linear combination of seven Legendre polynomials with randomly selected coefficients, projected from -1 to $+1$ onto the 40 s time interval and initialized to a random seed value at the start of each experiment. As reported in our previous study (Zotev et al., 2018a), this random feedback appeared to provide meaningful real-time information, although the waveform's shape was random, and varied randomly across condition blocks and subjects. Subjects were assigned to either EG or CG indiscriminately. Since one of the purposes of this study was to examine the feasibility of controlling brain activation using rtfMRI-nf, subjects in CG were unaware of the sham feedback, and they performed the same training and task sequence as EG participants.

The consensus on the reporting and experimental design of clinical and cognitive-behavioral neurofeedback studies (CRED-nf checklist) (Ros et al., 2019) was included in the supplementary section.

In order to assist participants to recall their important thoughts and think about them before the scan, we asked them to fill out the Portrait Values Questionnaire (PVQ) questionnaire. The PVQ has nine sections. Each section includes the Value Domains (areas of your life you may find important) listed as follows (Flaxman et al., 2011): (a) family relationships; (b) friendships/social relationships; (c) couples/romantic relationships; (d) work/career; (e) education-schooling/personal growth and development; (f) recreation/leisure/sport; (g) spirituality/religion; (h) community/citizenship; and (i) health/physical well-being. This survey was assigned to subjects to help them to come up with five things that are important to them.

2.4 | Data processing and analysis

AFNI (<http://afni.nimh.nih.gov>) (Cox & Hyde, 1997) was used for image data analysis. The first 23 fMRI volumes were discarded to

exclude the first three TR and the initial rest period from the analysis before applying any further analysis. fMRI data preprocessing included despiking, RETROICOR (Glover et al., 2000), respiration volume per time correction (Birn et al., 2008), slice-timing and motion corrections, nonlinear warping to the Montreal Neurological Institute (MNI) template brain with resampling to 2 mm³ voxels using the Advanced Normalization Tools software (Avants et al., 2009) (<http://stnava.github.io/ANTs/>), spatial smoothing with a 6 mm FWHM Gaussian kernel, and scaling signal to percent change relative to the mean in each voxel. The general linear model (GLM) analysis was used for evaluating the brain response in the RE, PR, NF-1, NF-2, NF-3, and TR runs. The design matrix included a modeled response to the Think block (boxcar function convolved with hemodynamic response function), 12 motion parameters (3 shift and 3 rotation parameters with their temporal derivatives), three principal components of the ventricle signal, local white matter average signal (ANATICOR) (Jo et al., 2010), and low-frequency fluctuation (fourth-order Legendre polynomial model). The GLM analysis was performed for each RE, PR, NF-1, NF-2, NF-3, and TR runs independently. The beta coefficient of the Think block regressor was extracted to estimate brain activation during the neurofeedback period and then converted to percent signal changes for Think versus Count contrast.

We examined the training effect on whole brain activation during the neurofeedback period (i.e., among PR, NF-1, NF-2, and NF-3 runs) using linear mixed-effect (LME) model analysis for longitudinal effects. The *lme4* package (Bates et al., 2014) in R language and statistical computing (R Core Team, 2016) were used. The LME model included fixed effects of neurofeedback run (as a numerical variable of 0–3 corresponding to PR, NF-1, NF-2, and NF-3), group (EG and CG), a group*run interaction, and a random effect of the subject on the intercept. Degrees of freedom for *F*-values were estimated by Satterthwaite's approximation in *lmerTest* package (Kuznetsova et al., 2017). The mean signal in each group was evaluated with *lsmeans* package (Lenth, 2016). The analysis was performed for each voxel, and the statistical map was thresholded with voxel-wise $p < .001$ and cluster-size corrected $p < .05$. Cluster-size threshold was evaluated with AFNI's 3dClustSim using an improved spatial autocorrelation function, a minimum cluster size of 75 voxels was required to have a corrected $p < .05$ with two-sided thresholding).

In addition, we used the real-time vmPFC ROI neurofeedback time series as a regressor in another GLM analysis to achieve a whole-brain map of BOLD signal correlation with the neurofeedback signal. All the coordinates presented in the rest of this work are referred to in MNI space unless otherwise noted. Statistical analyses were performed using MATLAB 2016b (MathWorks Inc., <http://www.mathworks.com/>) and Statistical Package for Social Sciences (IBM SPSS Statistics 23).

3 | RESULTS

Figure 2 shows the average BOLD signal (percentage signal changes for Think compared to Count) at the vmPFC neurofeedback target

region in each run for EG (in gray) and CG (in orange); the error bars present the standard error (SE) of the mean across participants. Groups did not differ significantly in vmPFC signal change across RE, PR, NF-1, NF-2, or NF-3 runs. Signal change (i.e., Think versus Count condition) in the target ROI was statistically significantly larger than zero for EG for all runs (RE: $t(17) = 7.799$, $p < 5e-7$; PR: $t(17) = 2.607$, $p < .018$; NF-1: $t(17) = 2.179$, $p < .044$; NF-2: $t(17) = 2.564$, $p < .020$; NF-3: $t(17) = 2.919$, $p < .012$; TR: $t(17) = 4.782$, $p < 2e-4$); In CG, signal change differed from zero only for RE and TR runs when no neurofeedback was given, whereas in any of the four neurofeedback runs, PR, NF-1, NF-2, or NF-3 signal change was not different from zero (RE: $t(8) = 4.159$, $p < .003$; PR: $t(8) = 1.092$, $p < .306$; NF-1: $t(8) = 0.418$, $p < .687$; NF-2: $t(8) = 0.389$, $p < .707$; NF-3: $t(8) = -0.228$, $p < .825$; TR: $t(8) = 3.257$, $p < .012$). The statistical details of the BOLD signal change are shown in Supplementary Table 1. Cohen's effect size and power were calculated with free software Gpower (v.3.1.9) (Faul et al., 2009).

Figure 3 shows the mean activation (Think–Count) fMRI contrast during the neurofeedback runs (PR, NF-1, NF-2, and NF-3) for EG. This map indicates that this internal self-regulation task recruited several other brain areas like middle frontal gyrus, inferior frontal gyrus, insula, left precuneus, and others, and was not limited to the vmPFC. Supplementary Table 2 shows the coordinates of the peak activation network for the Think–Count fMRI contrast in EG.

We further investigated which other brain areas were associated with the signal change in the vmPFC that was used as the neurofeedback signal centered at (–2, 39, and –4 in MNI). Figure 4 shows the correlation map with the vmPFC ROI real-time neurofeedback signal within EG. The map indicated that not only the vmPFC but also several other DMN regions, such as precuneus and inferior parietal lobule, were correlated with the

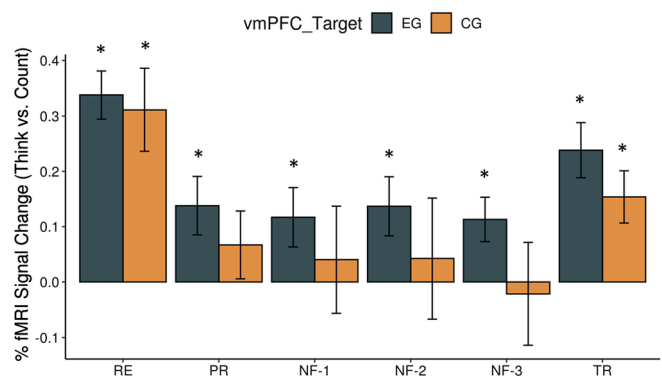


FIGURE 2 Percent fMRI BOLD signal change for the target ROI. The mean percent signal change for the Think–Count conditions for each experimental run: Practice (PR), Neurofeedback-1 (NF-1), Neurofeedback-2 (NF-2), and Neurofeedback-3 (NF-3) in the BOLD signal for targeted ventromedial prefrontal cortex (vmPFC: –2, 39, and –4). The error bars represent the SE of the mean. Supplementary Table 1 includes the mean BOLD signal changes and statistic results for RE, PR, NF-1, NF2, NF-3, and TR runs and both the subject groups. The asterisks show statistically significant difference from zero

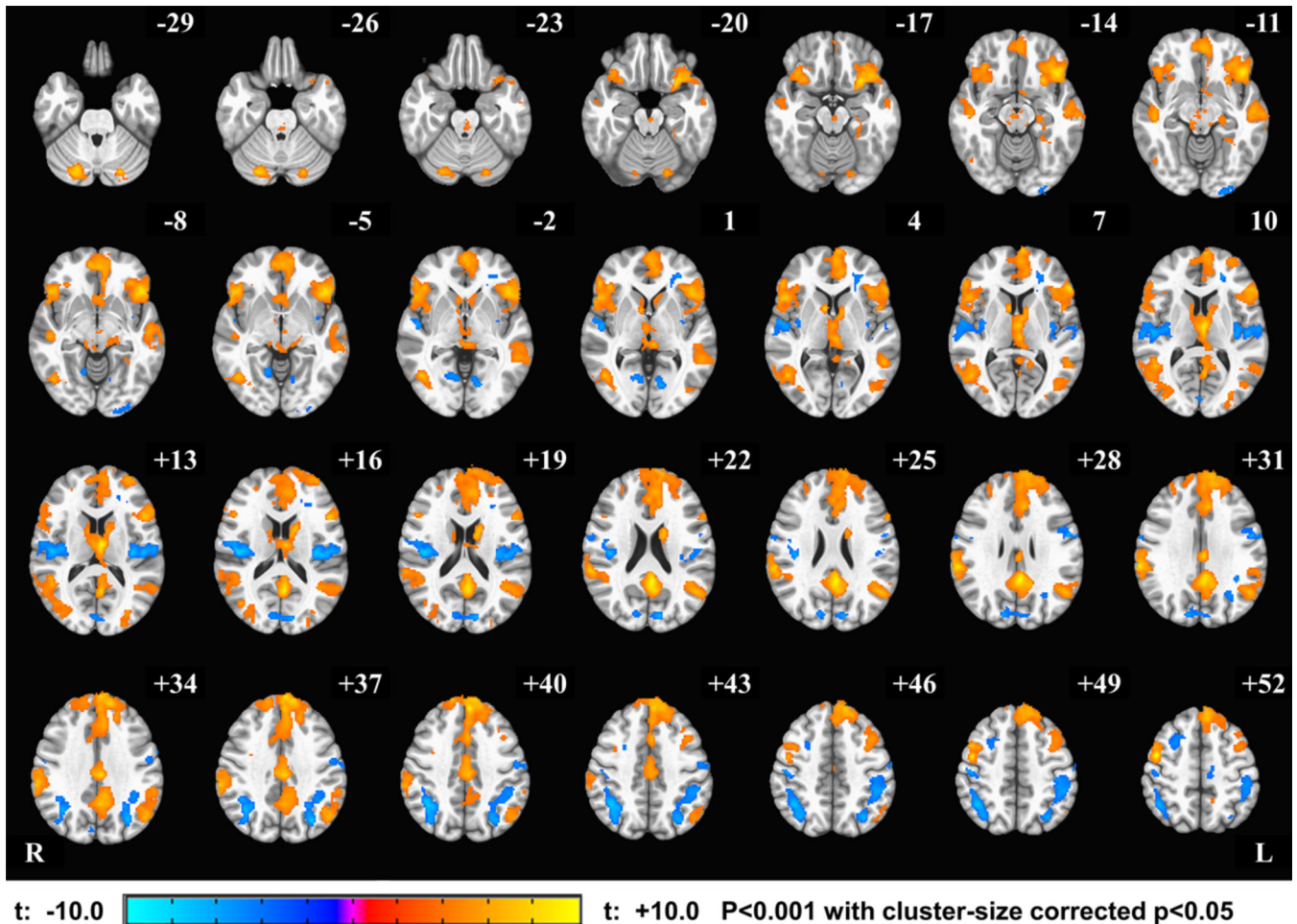


FIGURE 3 Activation Network for Think-Count condition within the experimental group (EG). The group fMRI activation analysis for the Think-Count contrast revealed significant positive BOLD signal changes in the DMN including vmPFC, precuneus, and right inferior parietal lobule, while the significant negative activations in insula and parietal lobe (see Supplementary Table 2 for clusters peak coordinates). The activation maps are projected on the MNI152 standard-space T1-weighted average structural template. The right side (R) of the brain is shown on the left, and the left side (L) is shown on the right

vmPFC neurofeedback signal (Supplementary Table 3 shows the significant clusters peak coordinates and identified brain regions).

Figure 5 shows brain regions indexing significant longitudinal effects of the training (linear trend across neurofeedback runs) within EG. Interestingly, we found only negative longitudinal effects of the training. Peak coordinates in each significant cluster are shown in Table 1. The largest cluster was seen in the dorsomedial prefrontal cortex, although right middle temporal gyri, right inferior frontal gyri, and left precuneus also showed decreasing trends across the training. Notably, no significant longitudinal effect was seen for CG. We did not find any significant clusters for group main effect, while the group*run interaction showed significant clusters in bilateral inferior frontal gyrus.

4 | DISCUSSION

We examined the feasibility of self-regulation of vmPFC activity with fMRI neurofeedback training. The vmPFC is a critical brain region, as

it is involved in several important processes, such as emotion, decision-making, and effective foresight. It is also part of the DMN. Since the DMN is known to be antagonistic to task-positive activation, tasks involved during neurofeedback training could decrease resting state DMN activity, including vmPFC. To modulate vmPFC activity, our fMRI-nf vmPFC training utilized both a self-relevant value-based thinking task and a self-regulation task in controlling the neurofeedback visual display (i.e., controlling red bar height, reflecting the signal level of vmPFC hemodynamic activity to match intended signal level as represented by a fixed target in a blue bar).

We predicted that the vmPFC percentage signal change (Think versus Count contrast) would increase from its baseline (RE) during neurofeedback runs in the EG as compared with CG. Instead, we found that the vmPFC signal was lower in both EG and CG during neurofeedback runs than at RE. This indicated that the self-relevant value-based thinking task might be enough to recruit the vmPFC and maintain its activity on a higher level than during the Count condition for the recall run. A lower vmPFC signal level during neurofeedback

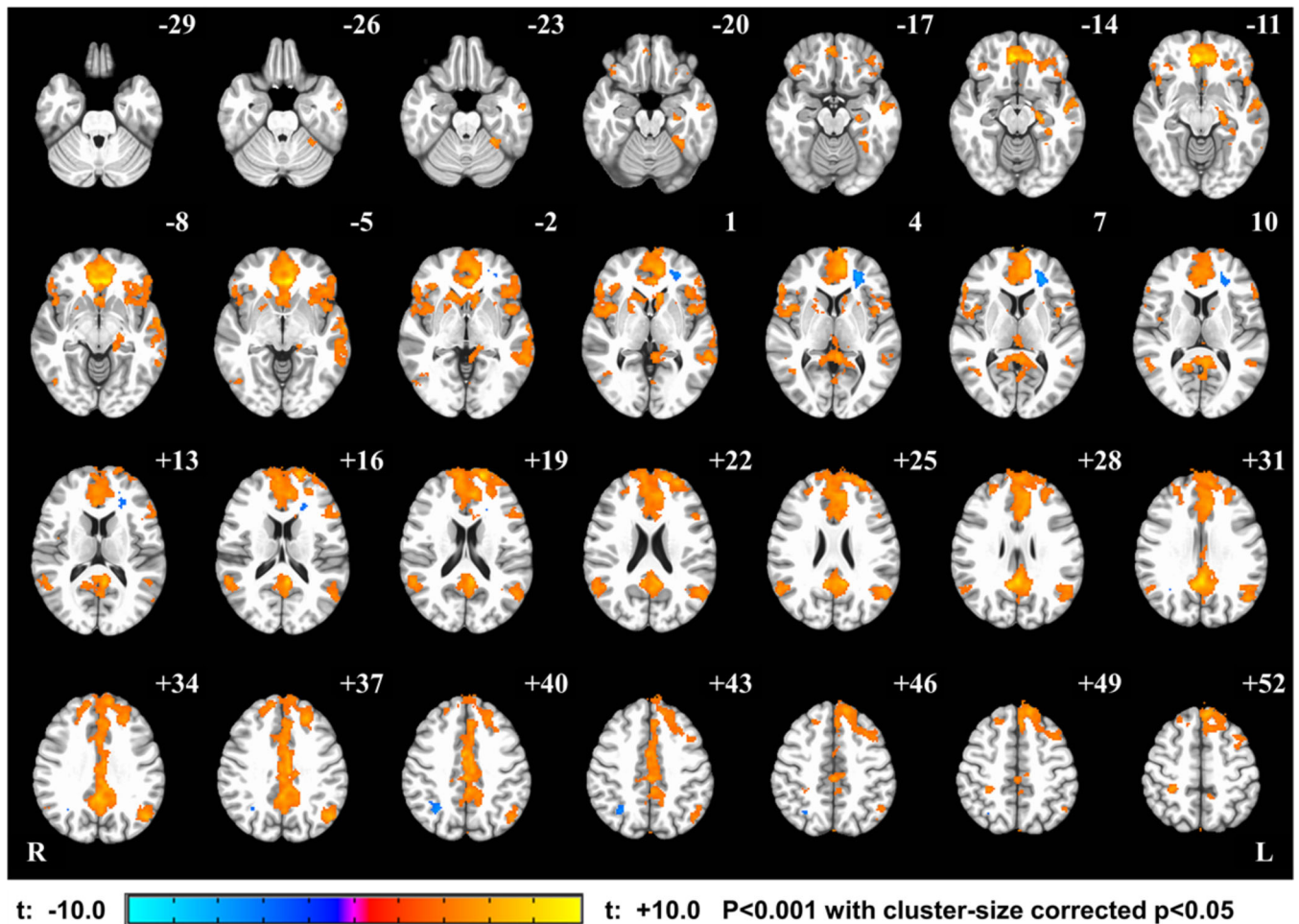


FIGURE 4 Real-time neurofeedback correlation map across experimental group (EG). The real-time feedback from vmPFC target during Think blocks was used as a regressor in fMRI GLM analysis among neurofeedback runs. This figure shows strong correlation between the real-time feedback and all brain regions in DMN, including vmPFC, precuneus, and right inferior parietal lobule (see Supplementary Table 3 for clusters peak coordinates)

runs can be attributed to the fact that the self-regulation task with neurofeedback, including attentional focus (i.e., the red bar), and the controlling tasks required to control external visual signal (i.e., red bar height control in PR, NF-1, NF-2, and NF-3) were distracting the participants (e.g., further suppressing DMN activity). As a result, participants were not able to maintain elevated vmPFC activity observed at the baseline. This is also supported by our results demonstrating that: (a) Think-Count BOLD contrast with an internal self-regulation task during vmPFC neurofeedback runs recruited several other DMN areas coactivated with vmPFC and (b) the real-time vmPFC neurofeedback signal alone was correlated with DMN activity in multiple regions. These indicated that vmPFC was not activated independently, but instead as part of the DMN during the neurofeedback task. Our findings point out important caveats to the neurofeedback training design; in the context of the selected mental strategy, the feedback signal from a single region did not necessarily reflect the specific neural activity of the region. A self-regulation effort could interfere with the activity in the regions of DMN and complicate response from the neurofeedback targeted ROI, especially when the neurofeedback

target constitutes part of the DMN. In addition, a recent meta-analysis of a neurofeedback study (Emmert et al., 2016) indicated that the neurofeedback training could recruit many brain region's activations associated with the self-regulation task regardless of the target region (e.g., the anterior insula and the basal ganglia). Therefore, when the neurofeedback target is associated with response to a self-regulation task, the signal change could reflect the self-regulation task itself, not the neurofeedback signal.

The current result also indicates the importance of the baseline condition in the neurofeedback training study. If we did not have a baseline (RE) run, the result could be misleading in that the neurofeedback training was successful, as the vmPFC activity during the neurofeedback NF-1, NF-2, and NF-3 and TR runs was significantly different from zero for the EG group (Figure 2). Considering the possibility that the self-regulation task could interfere with neurofeedback target brain activity, it is imperative that researchers include a baseline run without self-regulation neurofeedback training in future rtfMRI-nf studies.

While a significant training effect was not seen in the vmPFC activity across neurofeedback runs (PR, NF-1, NF-2, and NF-3),

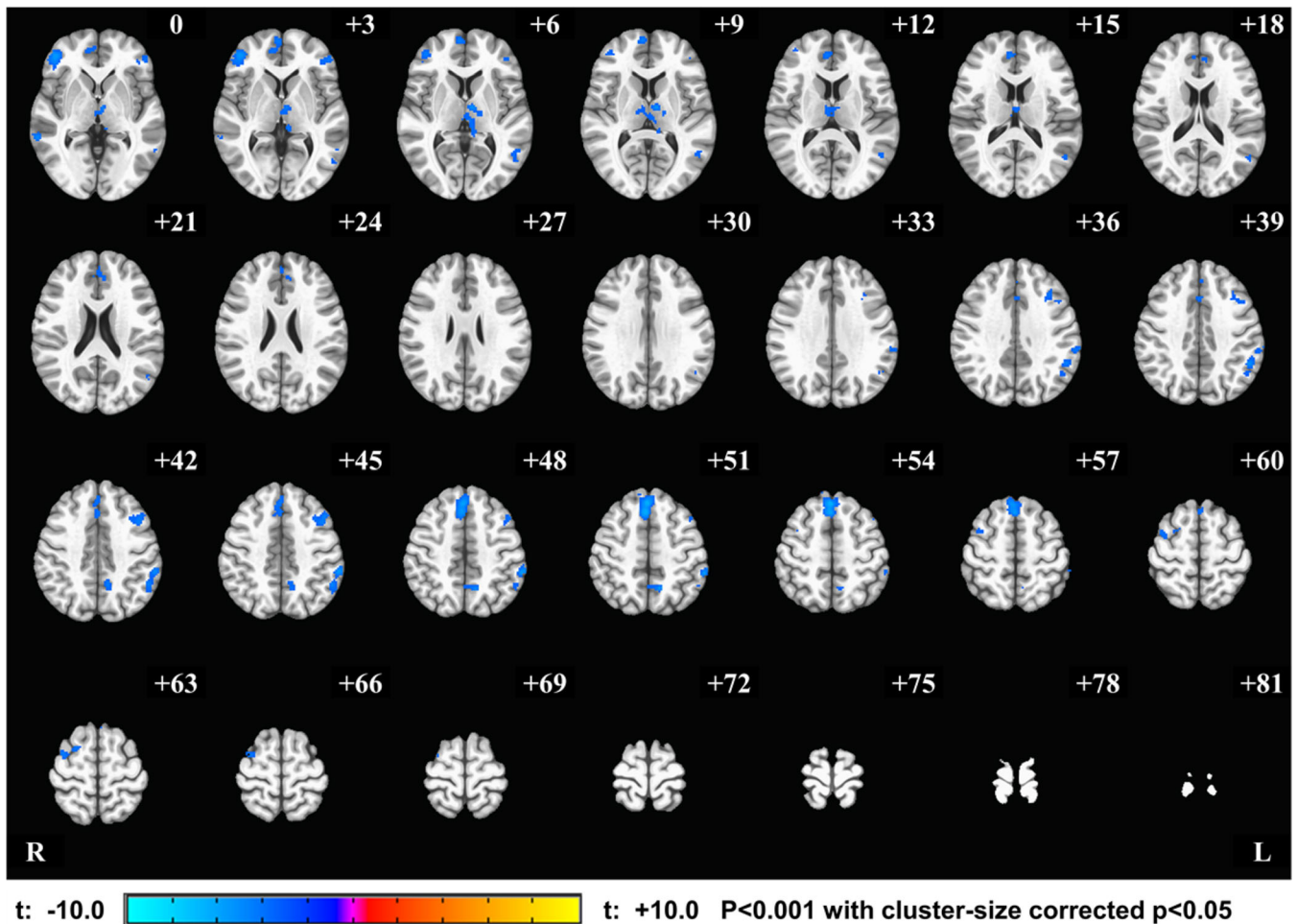


FIGURE 5 Longitudinal effect of rtfMRI-nf training within the experimental group (EG). The regions with the significant effect of run within EG were mapped on the MNI template brain. Negative value indicates that the signal of these regions linearly decreased across the neurofeedback training runs (PR, NF-1, NF-2, and NF-3). Peak coordinates for significant clusters are shown in Table 1

TABLE 1 Peak coordinates for clusters related to longitudinal analysis among neurofeedback runs for the experimental group (EG) ($p < .05$ corrected)

	Cluster			# voxels	t-score
	Peak coordinate (MNI)				
	x	y	z		
Right medial prefrontal cortex	1	35	53	573	-6.79
Left inferior parietal lobule	-61	-37	47	345	-6.03
Thalamus	-7	-9	7	298	-5.22
Right inferior frontal gyrus	45	45	1	271	-5.62
Left middle frontal gyrus	-45	19	45	235	-4.64
Right middle temporal gyrus	65	-27	-5	191	-5.81
Lobule VI, VIIa, Crus I	-15	-79	-25	137	-4.82
Right medial frontal gyrus	7	47	15	126	-4.28
Left precuneus	-11	-55	51	122	-5.4
Right medial frontal gyrus	5	61	5	117	-4.78
Left inferior frontal lobule	-49	41	3	106	-4.34
Right middle frontal gyrus	35	1	65	105	-4.64
Left middle temporal gyrus	-51	-59	11	101	-4.09

Abbreviation: MNI, Montreal Neurological Institute space.

several brain regions, including the medial prefrontal cortex, right middle temporal gyri, right inferior frontal gyri, and left precuneus, showed a decreasing trend across the training runs only for the EG (Figure 5). Several studies report correlations between deactivation of these brain regions and successful neurofeedback learning (Ninaus et al., 2013; Radua et al., 2018; Reiner et al., 2018). These suggest that EG could learn to accommodate the demand of the self-regulation task to maintain vmPFC activity with the help of a neurofeedback signal.

The original motivation of the vmPFC self-regulation training was to strengthen a healthy individual's ability to better cope with stressful events. We also considered that it might have an application for individuals with mood and anxiety disorders. However, the caveat raised in the current study indicates that vmPFC could coactivate with DMN at least in the current task context (focusing on thought about what is important). Abnormal increase of DMN activity has been observed for patients with MDD, and such an activity increase was specifically associated with depressive symptoms (Hamilton et al., 2011; Hamilton et al., 2015; Mulders et al., 2015; Williams, 2017). Therefore, any intervention resulting in increasing DMN activity could be rather harmful in treating MDD patients. As such, we must exercise caution when interpreting the functional meaning of the neurofeedback signal, especially when it is aimed to be used for treating a patient. The vmPFC activity could promote stress coping in one context, but it could worsen MDD pathology in another context when it is coactivated with DMN.

Finally, this study emphasizes the fact that sole brain activation cannot specify function by itself. When designing neurofeedback treatment, we must investigate what brain activations are associated with intended neurofeedback signal modulation and among neurofeedback training in the entire brain. The specificity of the neurofeedback signal's association with the neurofeedback target region is not trivial.

5 | CONCLUSIONS

We investigated the feasibility of targeting vmPFC fMRI neurofeedback in healthy individuals. Self-regulation of vmPFC activity with neurofeedback shows several caveats of neurofeedback training. The neurofeedback signal from the vmPFC was associated with whole DMN activity. In addition, the effort of self-regulation decreased the vmPFC activity as a part of DMN. Further investigation is required to learn accommodating competing task demands and the DMN activity. Findings from this study indicate the importance of functional specificity of the neurofeedback signal in achieving targeted effects. In addition, the neurofeedback signal from a single region might not necessarily be specifically localized to that region. Therefore, it is also important to evaluate coactivated regions with a neurofeedback signal and the functional meaning of those coactivations. This would also help to properly design neurofeedback training for clinical applications, aiming to correct specific brain functional abnormalities and improve clinical symptoms in patients with mental disorders.

ACKNOWLEDGMENTS

We are grateful to Julie Owen, Bill Alden, Julie DiCarlo, and Greg Hammond for helping with collecting neuroimaging MRI/fMRI data. The study was supported by the Laureate Institute for Brain Research and William K. Warren Foundation, and in part by the 1P20GM121312 award from the National Institute of General Medical Sciences and the National Institutes of Health.

CONFLICT OF INTERESTS

The authors declare that the research was conducted in the absence of any commercial or financial relationships that could be construed as a potential conflict of interest.

DATA AVAILABILITY STATEMENT

The data that support the findings of this study are available from the corresponding author upon reasonable request

ORCID

Jerzy Bodurka  <https://orcid.org/0000-0003-0053-9746>

REFERENCES

- Avants, B. B., Tustison, N., & Song, G. (2009). Advanced normalization tools (ANTS). *Insight Journal*, 2, 1–35.
- Bartra, O., McGuire, J. T., & Kable, J. W. (2013). The valuation system: A coordinate-based meta-analysis of BOLD fMRI experiments examining neural correlates of subjective value. *NeuroImage*, 76, 412–427.
- Bates, D., Mächler, M., Bolker, B., and Walker, S. (2014). Fitting linear mixed-effects models using lme4. *arXiv preprint arXiv:1406.5823*.
- Bechara, A., Damasio, H., Tranel, D., & Damasio, A. R. (1997). Deciding advantageously before knowing the advantageous strategy. *Science*, 275, 1293–1295.
- Bechara, A., Tranel, D., & Damasio, H. (2000). Characterization of the decision-making deficit of patients with ventromedial prefrontal cortex lesions. *Brain*, 123, 2189–2202.
- Bechara, A., Tranel, D., Damasio, H., & Damasio, A. R. (1996). Failure to respond autonomously to anticipated future outcomes following damage to prefrontal cortex. *Cerebral Cortex*, 6, 215–225.
- Benoit, R. G., Szpunar, K. K., & Schacter, D. L. (2014). Ventromedial prefrontal cortex supports affective future simulation by integrating distributed knowledge. *Proceedings of the National Academy of Sciences*, 111, 16550–16555.
- Berman, B. D., Horowitz, S. G., & Hallett, M. (2013). Modulation of functionally localized right insular cortex activity using real-time fMRI-based neurofeedback. *Frontiers in Human Neuroscience*, 7, 638.
- Berman, B. D., Horowitz, S. G., Venkataraman, G., & Hallett, M. (2012). Self-modulation of primary motor cortex activity with motor and motor imagery tasks using real-time fMRI-based neurofeedback. *NeuroImage*, 59, 917–925.
- Bhanji, J. P., & Delgado, M. R. (2014). Perceived control influences neural responses to setbacks and promotes persistence. *Neuron*, 83, 1369–1375.
- Birn, R. M., Smith, M. A., Jones, T. B., & Bandettini, P. A. (2008). The respiration response function: The temporal dynamics of fMRI signal fluctuations related to changes in respiration. *NeuroImage*, 40, 644–654.

- Bodurka, J., & Bandettini, P. (2008). Real-time software for monitoring MRI scanner operation. *NeuroImage*, 41, S85.
- Brosch, T., & Sander, D. (2013). Neurocognitive mechanisms underlying value-based decision-making: From core values to economic value. *Frontiers in Human Neuroscience*, 7, 398.
- Burghy, C. A., Stodola, D. E., Ruttler, P. L., Molloy, E. K., Armstrong, J. M., Oler, J. A., ... Birn, R. M. (2012). Developmental pathways to amygdala-prefrontal function and internalizing symptoms in adolescence. *Nature Neuroscience*, 15, 1736–1741.
- Caria, A., Sitaram, R., Veit, R., Begliomini, C., & Birbaumer, N. (2010). Volitional control of anterior insula activity modulates the response to aversive stimuli. A real-time functional magnetic resonance imaging study. *Biological Psychiatry*, 68, 425–432.
- Caria, A., Veit, R., Sitaram, R., Lotze, M., Weiskopf, N., Grodd, W., & Birbaumer, N. (2007). Regulation of anterior insular cortex activity using real-time fMRI. *NeuroImage*, 35, 1238–1246.
- Christopher Decharms, R. (2008). Applications of real-time fMRI. *Nature Reviews Neuroscience*, 9, 720–729.
- Christopher Decharms, R., Maeda, F., Glover, G. H., Ludlow, D., Pauly, J. M., Soneji, D., ... Mackey, S. C. (2005). Control over brain activation and pain learned by using real-time functional MRI. *Proceedings of the National Academy of Sciences of the United States of America*, 102, 18626–18631.
- Clithero, J. A., & Rangel, A. (2013). Informatic parcellation of the network involved in the computation of subjective value. *Social Cognitive and Affective Neuroscience*, 9, 1289–1302.
- Cox, R. W., & Hyde, J. S. (1997). Software tools for analysis and visualization of fMRI data. *NMR in Biomedicine*, 10, 171–178.
- Cox, R. W., & Jesmanowicz, A. (1999). Real-time 3D image registration for functional MRI. *Magnetic Resonance in Medicine*, 42, 1014–1018.
- Damasio, A. R. (1996). The somatic marker hypothesis and the possible functions of the prefrontal cortex. *Philosophical Transactions of the Royal Society B*, 351, 1413–1420.
- Emmert, K., Kopel, R., Sulzer, J., Brühl, A. B., Berman, B. D., Linden, D. E., ... Frank, S. (2016). Meta-analysis of real-time fMRI neurofeedback studies using individual participant data: How is brain regulation mediated? *NeuroImage*, 124, 806–812.
- Faul, F., Erdfelder, E., Buchner, A., & Lang, A.-G. (2009). Statistical power analyses using G* Power 3.1: Tests for correlation and regression analyses. *Behavior Research Methods*, 41, 1149–1160.
- Flaxman, P. E., Blackledge, J. T., & Bond, F. W. (2011). *Acceptance and commitment therapy: Distinctive features*. New York, NY: Routledge.
- Glover, G. H., Li, T. Q., & Ress, D. (2000). Image-based method for retrospective correction of physiological motion effects in fMRI: RETRO-ICOR. *Magnetic Resonance in Medicine: An Official Journal of the International Society for Magnetic Resonance in Medicine*, 44, 162–167.
- Haller, S., Kopel, R., Jhooti, P., Haas, T., Scharnowski, F., Lovblad, K.-O., ... Van De Ville, D. (2013). Dynamic reconfiguration of human brain functional networks through neurofeedback. *NeuroImage*, 81, 243–252.
- Hamilton, J. P., Farmer, M., Fogelman, P., & Gotlib, I. H. (2015). Depressive rumination, the default-mode network, and the dark matter of clinical neuroscience. *Biological Psychiatry*, 78, 224–230.
- Hamilton, J. P., Furman, D. J., Chang, C., Thomason, M. E., Dennis, E., & Gotlib, I. H. (2011). Default-mode and task-positive network activity in major depressive disorder: Implications for adaptive and maladaptive rumination. *Biological Psychiatry*, 70, 327–333.
- Hare, T. A., Camerer, C. F., & Rangel, A. (2009). Self-control in decision-making involves modulation of the vmPFC valuation system. *Science*, 324, 646–648.
- Hiser, J., & Koenigs, M. (2018). The multifaceted role of the ventromedial prefrontal cortex in emotion, decision making, social cognition, and psychopathology. *Biological Psychiatry*, 83, 638–647.
- Janowski, V., Camerer, C., & Rangel, A. (2012). Empathic choice involves vmPFC value signals that are modulated by social processing implemented in IPL. *Social Cognitive and Affective Neuroscience*, 8, 201–208.
- Jo, H. J., Saad, Z. S., Simmons, W. K., Milbury, L. A., & Cox, R. W. (2010). Mapping sources of correlation in resting state fMRI, with artifact detection and removal. *NeuroImage*, 52, 571–582.
- Johnston, S. J., Boehm, S. G., Healy, D., Goebel, R., & Linden, D. E. (2010). Neurofeedback: A promising tool for the self-regulation of emotion networks. *NeuroImage*, 49, 1066–1072.
- Johnstone, T., Van Reekum, C. M., Urry, H. L., Kalin, N. H., & Davidson, R. J. (2007). Failure to regulate: Counterproductive recruitment of top-down prefrontal-subcortical circuitry in major depression. *The Journal of Neuroscience*, 27, 8877–8884.
- Kuznetsova, A., Brockhoff, P. B., & Christensen, R. H. B. (2017). lmerTest package: Tests in linear mixed effects models. *Journal of Statistical Software*, 82, 1–26.
- Lenth, R. V. (2016). Least-squares means: The R package lsmeans. *Journal of Statistical Software*, 69, 1–33.
- Mcdonald, A. R., Muraskin, J., Van Dam, N. T., Froehlich, C., Puccio, B., Pellman, J., ... Calhoun, V. D. (2017). The real-time fMRI neurofeedback based stratification of default network regulation neuroimaging data repository. *NeuroImage*, 146, 157–170.
- Milad, M. R., Pitman, R. K., Ellis, C. B., Gold, A. L., Shin, L. M., Lasko, N. B., ... Rauch, S. L. (2009). Neurobiological basis of failure to recall extinction memory in posttraumatic stress disorder. *Biological Psychiatry*, 66, 1075–1082.
- Mulders, P. C., Van Eijndhoven, P. F., Schene, A. H., Beckmann, C. F., & Tendolkar, I. (2015). Resting-state functional connectivity in major depressive disorder: A review. *Neuroscience & Biobehavioral Reviews*, 56, 330–344.
- Ninaus, M., Kober, S. E., Witte, M., Koschutnig, K., Stangl, M., Neuper, C., & Wood, G. (2013). Neural substrates of cognitive control under the belief of getting neurofeedback training. *Frontiers in Human Neuroscience*, 7, 914.
- Posse, S., Fitzgerald, D., Gao, K., Habel, U., Rosenberg, D., Moore, G. J., & Schneider, F. (2003). Real-time fMRI of temporolimbic regions detects amygdala activation during single-trial self-induced sadness. *NeuroImage*, 18, 760–768.
- Pruessmann, K. P., Weiger, M., Scheidegger, M. B., & Boesiger, P. (1999). SENSE: sensitivity encoding for fast MRI. *Magnetic resonance in medicine*, 42, 952–962.
- Radua, J., Stoica, T., Scheinost, D., Pittenger, C., & Hampson, M. (2018). Neural correlates of success and failure signals during neurofeedback learning. *Neuroscience*, 378, 11–21.
- Rance, M., Ruttorf, M., Nees, F., Schad, L. R., & Flor, H. (2014). Real time fMRI feedback of the anterior cingulate and posterior insular cortex in the processing of pain. *Human Brain Mapping*, 35, 5784–5798.
- R Core Team (2016). R: A language and environment for statistical computing. Vienna, Austria: R Found. Stat. Comput. Retrieved from <http://www.R-project.org/>
- Reiner, M., Gruzelier, J., Bamidis, P. D., & Auer, T. (2018). The science of neurofeedback: Learnability and effects. *Neuroscience*, 378, 1–10.
- Ros, T., Enriquez-Geppert, S., Zotev, V., Young, K., Wood, G., Whitfield-Gabrieli, S., Wan, F., Vialatte, F., Van De Ville, D., and Todder, D. (2019). Consensus on the reporting and experimental design of clinical and cognitive-behavioural neurofeedback studies (CRED-nf checklist).
- Scheinost, D., Stoica, T., Saksa, J., Papademetris, X., Constable, R., Pittenger, C., & Hampson, M. (2013). Orbitofrontal cortex neurofeedback produces lasting changes in contamination anxiety and resting-state connectivity. *Translational Psychiatry*, 3, e250.
- Sherwood, M. S., Kane, J. H., Weisend, M. P., & Parker, J. G. (2016). Enhanced control of dorsolateral prefrontal cortex neurophysiology with real-time functional magnetic resonance imaging (rt-fMRI) neurofeedback training and working memory practice. *NeuroImage*, 124, 214–223.

- Shibata, K., Watanabe, T., Sasaki, Y., & Kawato, M. (2011). Perceptual learning incepted by decoded fMRI neurofeedback without stimulus presentation. *Science*, *334*, 1413–1415.
- Simpson, J. R., Drevets, W. C., Snyder, A. Z., Gusnard, D. A., & Raichle, M. E. (2001). Emotion-induced changes in human medial prefrontal cortex: II. During anticipatory anxiety. *Proceedings of the National Academy of Sciences*, *98*, 688–693.
- Sinha, R., Lacadie, C. M., Constable, R. T., & Seo, D. (2016). Dynamic neural activity during stress signals resilient coping. *Proceedings of the National Academy of Sciences*, *113*, 8837–8842.
- Talairach, J., and Tournoux, P. (1988). Co-planar stereotaxic atlas of the human brain. 3-dimensional proportional system: An approach to cerebral imaging.
- Weiskopf, N., Veit, R., Erb, M., Mathiak, K., Grodd, W., Goebel, R., & Birbaumer, N. (2003). Physiological self-regulation of regional brain activity using real-time functional magnetic resonance imaging (fMRI): Methodology and exemplary data. *NeuroImage*, *19*, 577–586.
- Williams, L. M. (2017). Defining biotypes for depression and anxiety based on large-scale circuit dysfunction: A theoretical review of the evidence and future directions for clinical translation. *Depression and Anxiety*, *34*, 9–24.
- Yoo, S.-S., & Jolesz, F. A. (2002). Functional MRI for neurofeedback: Feasibility study on a hand motor task. *NeuroReport*, *13*, 1377–1381.
- Young, K. D., Siegle, G. J., Zotev, V., Phillips, R., Misaki, M., Yuan, H., ... Bodurka, J. (2017). Randomized clinical trial of real-time fMRI amygdala neurofeedback for major depressive disorder: Effects on symptoms and autobiographical memory recall. *American Journal of Psychiatry*, *174*, 748–755.
- Yu, H., Cai, Q., Shen, B., Gao, X., & Zhou, X. (2017). Neural substrates and social consequences of interpersonal gratitude: Intention matters. *Emotion*, *17*, 589–601.
- Zotev, V., Krueger, F., Phillips, R., Alvarez, R. P., Simmons, W. K., Bellgowan, P., ... Bodurka, J. (2011). Self-regulation of amygdala activation using real-time fMRI neurofeedback. *PLoS One*, *6*, e24522.
- Zotev, V., Misaki, M., Phillips, R., Wong, C. K., & Bodurka, J. (2018a). Real-time fMRI neurofeedback of the mediodorsal and anterior thalamus enhances correlation between thalamic BOLD activity and alpha EEG rhythm. *Human Brain Mapping*, *39*, 1024–1042.
- Zotev, V., Phillips, R., Misaki, M., Wong, C.K., Wurfel, B.E., Krueger, F., Feldner, M., and Bodurka, J. (2018b). Real-time fMRI neurofeedback training of the amygdala activity with simultaneous EEG in veterans with combat-related PTSD. *arXiv preprint arXiv: 1801.09165*.
- Zotev, V., Phillips, R., Yuan, H., Misaki, M., & Bodurka, J. (2014). Self-regulation of human brain activity using simultaneous real-time fMRI and EEG neurofeedback. *NeuroImage*, *85*, 985–995.

SUPPORTING INFORMATION

Additional supporting information may be found online in the Supporting Information section at the end of this article.

How to cite this article: Mayeli A, Misaki M, Zotev V, et al. Self-regulation of ventromedial prefrontal cortex activation using real-time fMRI neurofeedback—Influence of default mode network. *Hum Brain Mapp*. 2020;41:342–352. <https://doi.org/10.1002/hbm.24805>